How to cite: *Angew. Chem. Int. Ed.* **2021**, *60*, 13500–13506
International Edition: doi.org/10.1002/anie.202103427
German Edition: doi.org/10.1002/ange.202103427

Diboranes Hot Paper

B–B vs. B–H Bond Activation in a (μ-Hydrido)diborane(4) Anion upon Cycloaddition with CO_2, Isocyanates, or Carbodiimides

*Timo Trageser, Dariusz Bebej, Michael Bolte, Hans-Wolfram Lerner, and Matthias Wagner**

Abstract: *The intriguing (μ-hydrido)diboranes(4) with their prominent pristine representative $[B_2H_5]^-$ have mainly been studied theoretically. We now describe the behavior of the planarized tetraaryl (μ-hydrido)diborane(4) anion **[1H]**$^-$ in cycloaddition reactions with the homologous series of heterocumulenes CO_2, iPrNCO, and iPrNCNiPr. We show that a C=O bond of CO_2 selectively activates the B–B bond of **[1H]**$^-$, while the μ-H ligand is left untouched (**[2H]**$^-$). The carbodiimide iPrNCNiPr, in contrast, neglects the B–B bond and rather adds the B-bonded H^- ion to its central C atom to generate a formamidinate bridge across the B_2 pair (**[3]**$^-$). As a hybrid, the isocyanate iPrNCO combines the reactivity patterns of both its congeners and gives two products: one of them (**[4H]**$^-$) is related to **[2H]**$^-$, the other (**[5]**$^-$) is an analog of **[3]**$^-$. We finally propose a mechanistic scenario that rationalizes the individual reaction outcomes and combines them to a coherent picture of B–B vs. B–H bond activation.*

Introduction

The activation of C=E double bonds in (cyclo)addition reactions is the key step of countless organic syntheses (E = CR_2, NR, O). In the cases of corresponding C–E′ single bonds, however, more forcing reaction conditions and/or the addition of transition-metal catalysts are typically required (E′ = CR_3, NR_2, OR). Practically useful examples of single-bond activations have been reported predominantly for C–X (X = Cl, Br, I) or arene C–H bonds.[1]

Due to the smaller nuclear attraction potential of the boron atom compared to the carbon atom, the bonding orbitals of B–H and B–B single bonds are radially more extended and energetically higher than those of their C–H and C–C analogs.[2,3] This leads to increased reactivity, so that, for example hydroboration reactions can already occur spontaneously at room temperature.[4,5] As an important additional feature, boron atoms can easily expand their coordination numbers from c.n. = 3 to 4. Consequently, diboranes containing electron-precise B–B bonds are known with $B(sp^2)$–$B(sp^2)$, $B(sp^2)$–$B(sp^3)$, and $B(sp^3)$–$B(sp^3)$ cores. Such structural diversity allows for a fascinating variety of chemical conversions, as adduct formation does not per se have either a stabilizing or destabilizing influence on a diborane scaffold: The vacant $B(p_z)$ orbitals of diboranes(4) render their B–B bonds kinetically vulnerable. Coordination of a Lewis base can lead to kinetic protection, but, on the other hand, induces rehybridization of the boron center, thereby lengthening the B–B bond and again making it susceptible to cleavage. The ambiguity of Lewis-base coordination to diboranes(4) becomes immediately apparent when bis(pinacolato)diboron (B_2pin_2) is compared with parent B_2H_4: (i) While free B_2pin_2 is stable under ambient conditions, addition of KO*t*Bu leads to heterolytic cleavage of the B–B bond in presence of suitable substrates, which is widely exploited for borylation and diboration reactions.[6] (ii) Free B_2H_4 can only be investigated by low-temperature matrix spectroscopy (3 K; solid neon) and partially compensates for its electron deficiency by forming a doubly H-bridged C_{2v} structure.[7–9] Various ligands proved to be suitable for the preparation of diadducts $(L)H_2B–BH_2(L)$ that are sufficiently stable for X-ray crystallography and further derivatizations.[10] Obviously, the chemistry of B–B two-electron-two-center (2e2c) bonds is far from being well explored or fully understood and still holds many surprises.[11] Major drawbacks for further studies include a lack of efficient synthesis protocols and the dilemma that sterically demanding or π-donating substituents, which are often mandatory to obtain isolable compounds, inevitably impair also desired diborane-substrate interactions.

Conceptually, our group considers (μ-hydrido)diborane(4) anions as an ideal class of compounds to study the reactivity of B–B single bonds. The bridging H^- ion is the least sterically demanding ligand available to saturate both $B(p_z)$ orbitals simultaneously. Concurrently, H^- can easily shift to a terminal position, thereby exposing one tricoordinated boron center to nucleophilic attack. For the parent system $[B_2H_5]^-$, some knowledge has already been gained from experiments and quantum-chemical calculations: the anion was generated in an argon matrix at 8 K and its B–B bond was identified as a strong non-classical electron-donor site.[12,13] In an extreme view, $[B_2H_5]^-$ can be described as a protonated diborene, $H^+/[H_2B{=}BH_2]^{2-}$, which further underscores the pronounced donor potential of the B–B bond.[14,15] Despite their high promise for the discovery of fundamentally important reactivity patterns, isolable derivatives of $[B_2H_5]^-$ are virtually unknown, the only exception being Tamao's molecule, which bears two bulky

[*] M. Sc. T. Trageser, B. Sc. D. Bebej, Dr. M. Bolte, Dr. H.-W. Lerner, Prof. Dr. M. Wagner
Institut für Anorganische Chemie
Goethe-Universität Frankfurt
Max-von-Laue-Strasse 7, 60438 Frankfurt (Main) (Germany)
E-mail: Matthias.Wagner@chemie.uni-frankfurt.de
Supporting information and the ORCID identification number(s) for the author(s) of this article can be found under: https://doi.org/10.1002/anie.202103427.

1,1,3,3,5,5,7,7-octaethyl-*s*-hydrindacen-4-yl (Eind) substituents.[16,17]

We recently disclosed the synthesis of the tetraaryl (μ-hydrido)diborane(4) anion [**1**H]$^-$, which possesses a sterically exposed BHB three-membered ring. Its alkali-metal salts M[**1**H] ($M^+ = Li^+$–K^+) are available in near quantitative yields through deprotonation of the tetraaryl diborane(6) **1**H_2[18–25] using sterically demanding Brønsted bases ($LiC(SiMe_3)_3$, $NaN(SiMe_3)_2$, $KN(SiMe_3)_2$; Scheme 1).[15]

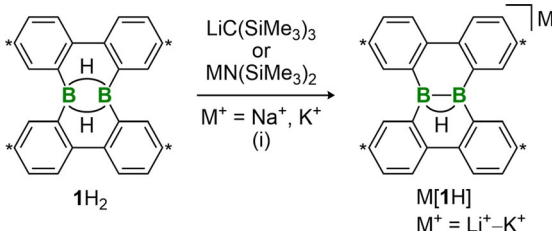

Scheme 1. Synthesis of organic $[B_2H_5]^-$ derivatives M[**1**H] through deprotonation of the B_2H_6 derivative **1**H_2; carbon atoms marked with asterisks bear *t*Bu substituents. (i) THF, room temperature.

Herein, we describe the highly selective reaction of M[**1**H] with the abundant C_1 building block CO_2 and with its analogs *i*PrNCO and *i*PrNCN*i*Pr. This substrate scope allows us to systematically assess how the steric demand of the heterocumulene together with subtle changes in its electronic structure influence the reaction pattern of the BHB core.

Results and Discussion

According to quantum-chemical calculations, [**1**H]$^-$ with its μ-H-supported B–B bond is the thermodynamically most favorable among several conceivable isomers.[5] Only 5.1 and 6.6 kcal mol^{-1} higher in energy lie the isomeric minimum structures [**1a**H]$^-$ and [**1b**H]$^-$, in which two formal Wagner–Meerwein rearrangements have converted the dibenzo-[*g*,*p*]chrysene-type scaffold of [**1**H]$^-$ into the 9,9′-difluorene-type frameworks of [**1a**H]$^-$ and [**1b**H]$^-$ (Figure 1a). While in [**1a**H]$^-$ the hydride substituent is located at a terminal position, it remains in a bridging mode in [**1b**H]$^-$. We already previously found evidence that [**1a**H]$^-$ is indeed thermally accessible at room temperature and does significantly contribute to the reactivity of the system.[5,26] The shift of the H$^-$ ligand between bridging and terminal positions decisively influences the nodal structures of the respective frontier orbitals such that [**1**H]$^-$/[**1b**H]$^-$ and [**1a**H]$^-$ can interact with an incoming heterocumulene in different ways. Four conceivable modes of interaction are exemplarily shown for CO_2 in Figure 1. The HOMO of [**1**H]$^-$/[**1b**H]$^-$ features lobes of π symmetry at its B–B bond[5] and can thus behave as a σ donor toward a CO_2 molecule approaching the B–B bond along a trajectory perpendicular to the bond vector (B–B bond activation). It becomes obvious that an overall constructive interaction with the LUMO of CO_2 should be possible, since the lobe at the central C atom (bonding interaction) is considerably larger than the lobes at the peripheral O atoms

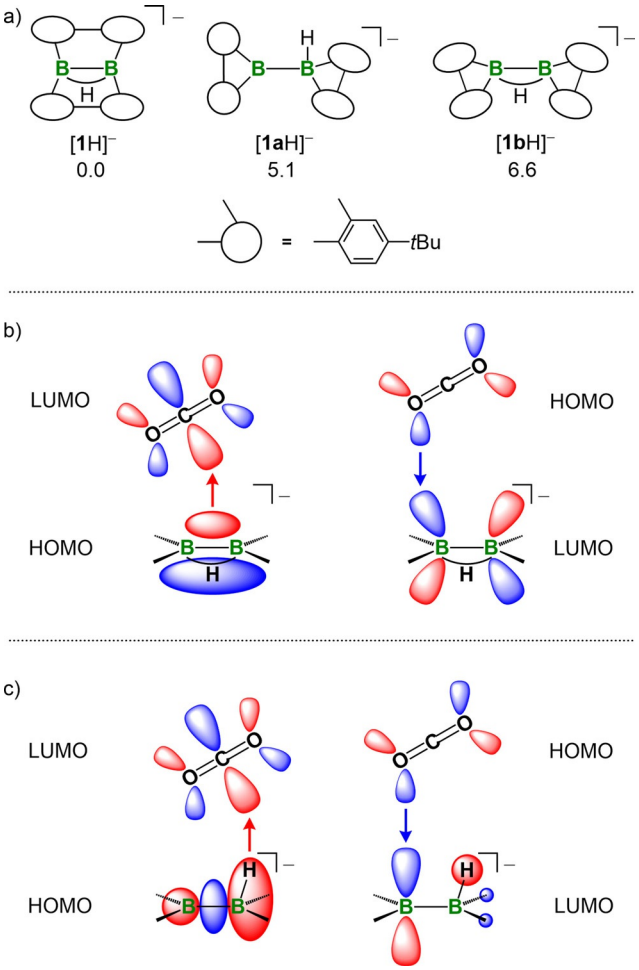

Figure 1. a) Schematic representations and relative Gibbs free energies [kcal mol^{-1}] of the three isomers [**1**H]$^-$ (dibenzo[*g*,*p*]chrysene-type) and [**1a**H]$^-$, [**1b**H]$^-$ (9,9′-difluorene-type). b) Possible frontier-orbital interactions between [**1**H]$^-$ or [**1b**H]$^-$ and the model heterocumulene CO_2. c) Possible frontier-orbital interactions between [**1a**H]$^-$ and the model heterocumulene CO_2.

(antibonding interactions; Figure 1b). Alternatively, the bonding B–H orbital of [**1a**H]$^-$ could act as the nucleophile toward the C atom of CO_2 (B–H bond activation; Figure 1c).[27] In any case, one of the O atoms is an ideally positioned Lewis base to form an adduct with the (resulting) tricoordinated B atom of [**1**H]$^-$/[**1a**H]$^-$/[**1b**H]$^-$. We will show that the B–B bond activation scenario is encountered with CO_2, the B–H bond activation scenario with *i*PrNCN*i*Pr, and both at the same time with *i*PrNCO.

The three substrates were treated with all three available alkali-metal salts M[**1**H] ($M^+ = Li^+$–K^+) in order to examine possible counter-cation effects, which have shown to be relevant for the reactivities of several comparable anionic boron compounds.[22,28–30]

Moreover, we employed initial reaction temperatures of both −78 °C and room temperature throughout to avoid relating products of kinetic reaction control to those of thermodynamic reaction control. In the present cases, the counter cations had little influence and the reaction temperature did not play any role. Therefore, we will mainly describe

the room-temperature reactions of K[**1**H] as this salt provided the most comprehensive set of information (differing behavior of Li[**1**H]/Na[**1**H] is mentioned where appropriate).

When a solution of K[**1**H] in [D_8]THF was placed under a blanket of CO_2 (1 atm), the initial intense yellow color faded immediately. NMR spectroscopy showed a quantitative conversion to one single product (K[**2**H]; Scheme 2a), which

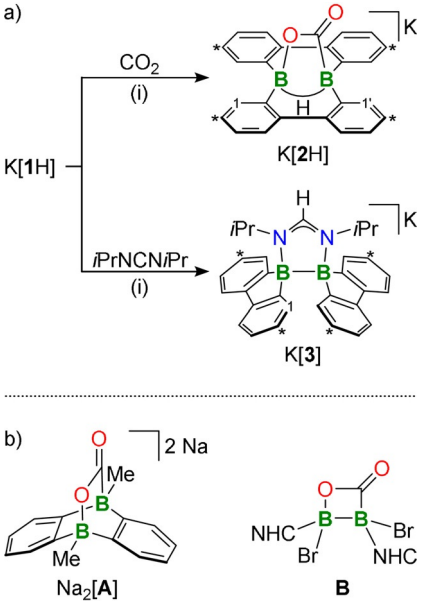

Scheme 2. a) Cycloaddition reactions between K[**1**H] and CO_2 or *i*PrNCN*i*Pr, furnishing the B–B activation product K[**2**H] or the B–H activation product K[**3**], respectively; carbon atoms marked with asterisks bear *t*Bu substituents. b) Model compounds Na_2[**A**] and **B** used for comparison; NHC = 1,3-bis(2,6-diisopropylphenyl)imidazol-2-ylidene. (i) [D_8]THF, room temperature.

could not be reverted to the starting materials through heating.[31] The ^{1}H and ^{13}C{^{1}H} NMR spectra of K[**2**H] are each characterized by two sets of signals of equal intensity, proving that the (on average) C_{2v} symmetry of the starting material K[**1**H] is broken in K[**2**H]. An extremely broad, unresolved proton signal, sharpening up upon ^{11}B decoupling, indicates that a B···B-bridging H^- ligand persists in K[**2**H]. However, the resonance now appears at $\delta(^1H) = 4.76$ ppm, almost 6 ppm downfield-shifted from the corresponding resonance of K[**1**H] ($\delta(^1H) = -0.99$ ppm),[22] which points toward a significantly altered electronic situation within the B(μ-H)B core. A low-field resonance at $\delta(^{13}C) = 195.5$ ppm is consistent with the presence of a B–O–C(O)–B fragment.[29,32] In line with that, two ^{11}B NMR resonances are found in the region of tetracoordinated boron nuclei ($\delta(^{11}B) = -1.6$, -5.1 ppm).[33]

X-ray crystallography on the centrosymmetric dimer {[K(pmdta)][**2**H]}$_2$·THF finally confirmed the molecular structure of the cycloaddition product (Figure 2; PMDTA: *N*,*N*,*N*′,*N*″,*N*″-pentamethyldiethylenetriamine; acronyms of coordinated solvent molecules are written in lowercase letters). The μ-H ligand was located in the difference Fourier map. Also, the proposed B–O–C(O)–B moiety was found; its

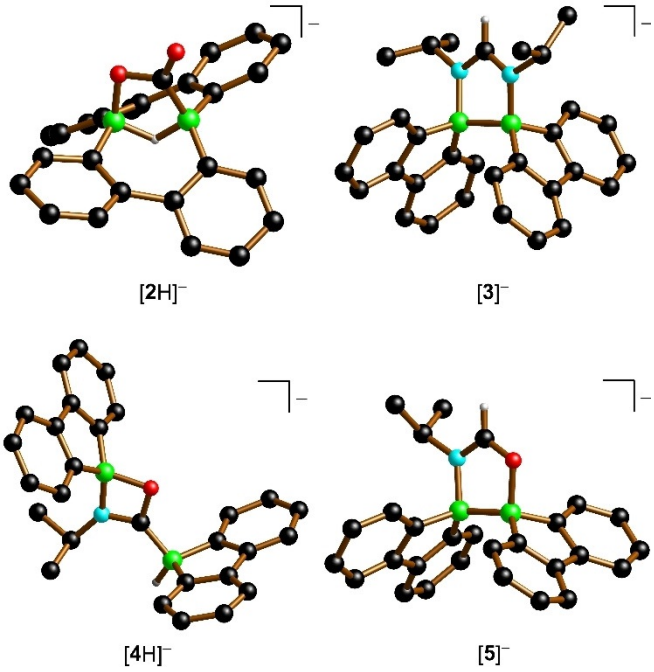

Figure 2. Solid-state structures of the anionic parts of {[K(pmdta)][**2**H]}$_2$·THF, [K(thf)$_2$][**3**], [K(dme)$_3$][K][**4**H]$_2$, and [Li(thf)$_3$][**5**]; most C-bonded H atoms and all *t*Bu substituents are omitted for clarity; B: green, C: black, H: gray, N: blue, O: red.

endocyclic O–C single bond has a length of 1.354(2) Å, while the exocyclic C=O double bond is significantly shorter (1.224(2) Å). The B–C and B–O bond lengths amount to 1.601(3) and 1.524(3) Å, respectively. We note that the B–O bond of K[**2**H], which is inert toward excess CO_2 over hours, is shorter by 0.065 Å than the B–O bond of a comparable cycloadduct Na_2[**A**] (Scheme 2b), which readily inserts a second molecule of CO_2.[29] Boron has a covalent radius of 0.84 Å.[34] While the B···B distance of the starting material [K(thf)$_2$][**1**H] (1.651(6) Å)[22] is within the binding regime, that of [**2**H]$^-$ falls clearly out of this range (2.141(3) Å). It is also instructive to compare [**2**H]$^-$ with **B** (Scheme 2b), a formal [2+2] cycloadduct of CO_2 with the B=B double bond of an NHC-supported diborene (NHC = 1,3-bis(2,6-diisopropylphenyl)imidazol-2-ylidene). **B** is described as still featuring a B–B single bond with a concomitant B···B distance of 1.80(2) Å.[35] To sum up, NMR and crystallographic data are in full agreement with the formal [2+2] cycloaddition of one C=O double bond of CO_2 across the B–B single bond of [**1**H]$^-$, whereupon this latter bond is broken and a central five-membered BOCBH heterocycle is constructed.

The addition of *i*PrNCN*i*Pr (1 equiv) to K[**1**H] in [D_8]THF resulted in the selective formation of K[**3**] (Scheme 2a). The ^{1}H NMR spectrum shows only one set of *t*Bu(C_6H_3) and *i*Pr signals with an overall integral ratio suggesting an equimolar reaction between the two starting materials. A resonance assignable to a B-bonded H atom is not detectable, even upon ^{11}B decoupling. Instead, we observe a singlet resonance at $\delta(^1H) = 8.07$ ppm (1H), showing a cross-peak to a signal at $\delta(^{13}C) = 158.8$ ppm in the ^{1}H-^{13}C HSQC experiment. The associated C–H moiety is obviously not part of an

aryl ring or an alkyl group, but can rather be assigned to a formic acid derivative.[36,37] Apart from the higher symmetry of K[**3**] compared to the CO_2 cycloadduct K[**2**H], a notable upfield shift of the resonance assignable to H-1 becomes evident (K[**3**]: 7.77 ppm vs. K[**2**H]: 8.15/8.04 ppm; cf. Scheme 2a). In our experience, the absence of aryl signals with chemical shift values of $\delta(^1H) > 8$ ppm in the spectrum of K[**3**] is a strong indication that this compound has a 9,9′-difluorene-type scaffold. Dibenzo[*g*,*p*]chrysene-type scaffolds, such as that of K[**2**H], consistently feature more deshielded H-1 protons due to the magnetic anisotropy effect prevalent in the cove regions[38] of polycyclic aromatic hydrocarbons.[39,40] The ^{11}B NMR spectrum of K[**3**] shows one signal at $\delta(^{11}B) = 0.7$ ppm; both B centers are thus chemically equivalent and tetracoordinated.[33]

X-ray diffraction on single crystals of $[K(thf)_2][\mathbf{3}]$ ultimately proved that the reaction of K[**1**H] with *i*PrNCN*i*Pr is indeed accompanied by two Wagner–Meerwein-type rearrangements (cf. Figure 2). The two B centers are spanned by a largely symmetrical formamidinate bridge (C–N = 1.319(5), 1.308(5) Å) and positioned at a distance of 1.821(6) Å. Thus, the five-membered BNCNB core of K[**3**] still contains a covalent B–B single bond.[34] The formamidinate-H atom originates from the previously B···B-bridging H^- ligand of K[**1**H], as confirmed by a deuteration experiment using K[**1**D] (NMR spectroscopic control). It is thus plausible to assume that the encounter complex between the two starting materials resembles the scenario outlined in Figure 1c for the model heterocumulene CO_2: We propose a charge flow from the bonding B–H orbital of the rearranged $[\mathbf{1a}H]^-$ to the LUMO of *i*PrNCN*i*Pr, accompanied by the formation of the first B–N bond. The second B–N adduct is formed at the newly generated tricoordinated B center after intramolecular rotation within the formamidinate ligand (Scheme 2a). The resulting B(sp^3)–B(sp^3) diborane salts M[**3**] ($M^+ = Li^+$–K^+) featuring a central five-membered BNCNB heterocycle are accessible in almost quantitative yields,[41] thus adding new members to a promising,[42] but experimentally little explored diborane class.[43]

In terms of electronic structure and steric demand, *i*PrNCO occupies an intermediate position between the two previously addressed substrate molecules. When it reacts with K[**1**H], two isomeric products are formed in competing reactions (Scheme 3a): K[**4**H] is related to the CO_2 adduct K[**2**H] (cf. Scheme 4), whereas K[**5**] is an analog of K[**3**]. According to ^1H NMR spectroscopy on the reaction mixture, K[**4**H] and K[**5**] are produced in a stoichiometric ratio of

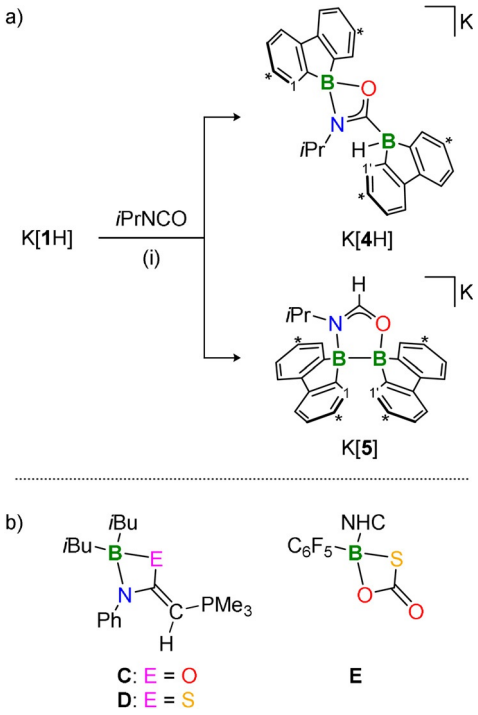

Scheme 3. a) Cycloaddition reaction between K[**1**H] and *i*PrNCO, furnishing both the B–B activation product K[**4**H] and the B–H activation product K[**5**]; carbon atoms marked with asterisks bear *t*Bu substituents. b) **C**–**E** are rare examples of structurally characterized boron compounds containing a chelate ligand related to that in K[**4**H]; NHC = *N*,*N*-dimesitylimidazol-2-ylidene. (i) $[D_8]$THF, room temperature.

1.5:1. Apart from a necessary symmetry break due to the switch from an NCN to an NCO bridge, the NMR data of K[**5**] do not differ significantly from those of K[**3**]. Importantly, the resonances of H-1/1′ (7.74/7.73 ppm) again appear below 8 ppm, in agreement with a 9,9′-difluorene-type molecule. The most revealing NMR features of the second product K[**4**H] are its two signals in the ^{11}B NMR spectrum: The first is broad and has a chemical shift value of $\delta(^{11}B) = 13.7$ ppm, the second appears as a doublet at $\delta(^{11}B) = -18.5$ ppm with a coupling constant $^1J(B,H) = 84$ Hz that is characteristic of a terminal H substituent.[33] The ^1H and $^{13}C\{^1H\}$ NMR spectra of K[**4**H] indicate the presence of two borafluorene units. Their chemical shift values are more pronouncedly different than in the case of K[**5**]; an assignment was achieved by means of a cross-peak between the ^{11}B doublet-resonance and the H-1′ signal in the ^1H-^{11}B HMBC experiment.

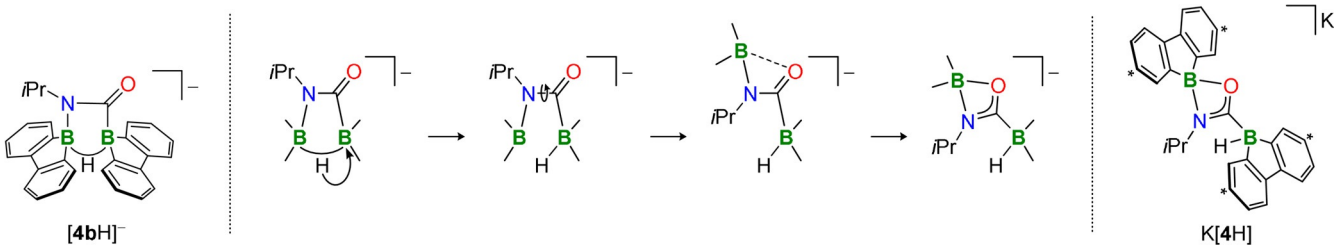

Scheme 4. The computed, energetically favorable primary product $[\mathbf{4b}H]^-$ of the cycloaddition reaction between K[**1**H] and *i*PrNCO and its rearrangement cascade to form K[**4**H]; carbon atoms marked with asterisks bear *t*Bu substituents.

We succeeded in the isolation of K[**4**H] through recrystallization of the blend of crude reaction products from a 1:1 mixture of THF:DME ([K(dme)$_3$][K][**4**H]$_2$; DME: 1,2-dimethoxyethane). Single crystals of [**5**]$^-$ could be grown in the form of its Li^+ salt [Li(thf)$_3$][**5**] (Figure 2). The molecular structure of [**5**]$^-$ is formally derived from the structure of [**3**]$^-$ by replacing one N*i*Pr moiety with an O atom to form a five-membered BNCOB heterocycle. The B–B (1.801(7) Å) and B–N bond lengths (1.605(6) Å) of [**5**]$^-$ are the same as those of [**3**]$^-$ within the experimental error margins; the length of the B–O bond is 1.652(6) Å. In the isomeric reaction product [**4**H]$^-$, the *i*PrNCO core is linked to one borafluorenyl substituent via a B–C bond and acts toward the other borafluorene as a κ^2-*N*,*O* chelating ligand (B–N = 1.586(6) Å, B–O = 1.570(6) Å). The B–O bond is considerably shorter (by 0.082 Å) than that of [**5**]$^-$, suggesting a stronger interaction, which may be one reason for the dominance of [**4**H]$^-$ over [**5**]$^-$ in the product mixture (note that the corresponding reaction with Na[**1**H] gives exclusively Na[**4**H]). On the other hand, [**4**H]$^-$ should suffer from considerable angular strain due to its four-membered ring structure, which may be one reason why related compounds, such as **C**–**E**, are very rare (Scheme 3b).[44] All in all, the preferential formation and stability of [**4**H]$^-$ remains astounding, given that Breher et al. explicitly mentioned that their compounds **C** and **D** are readily thermally decomposed.[44]

Quantum-chemical calculations were performed for all isomeric structure types [**2**H]$^-$–[**5**]$^-$.[45] Each structure type was computed with each of the three substrate fragments CO_2, *i*PrNCN*i*Pr, and *i*PrNCO (see the Supporting Information for graphical representations and Gibbs free energies of all computed structures). In the cases of CO_2 and *i*PrNCN*i*Pr, the energetically most favorable heterocyclic cores correspond to those found in the reaction products K[**2**H] and K[**3**], respectively. For *i*PrNCO, [**4**H]$^-$ represents the global minimum ($\Delta G = 0$); [**5**]$^-$ is higher in energy by only $\Delta G = +4.5$ kcal mol^{-1}. Energetically in between lies the isomer [**4b**H]$^-$ ($\Delta G = +2.7$ kcal mol^{-1}; Scheme 4), which has not been observed, likely because it rearranges to [**4**H]$^-$ without significant activation barrier: We assume that *i*PrNCO is not necessarily attacked by the B–H bond of [**1a**H]$^-$, but can alternatively activate the B–B bond of the energetically comparable B(μ-H)B isomer [**1b**H]$^-$ (Figure 1a) from the side opposite to the bridging H^- ligand. The BNCBH core in the resulting primary product [**4b**H]$^-$ is a structural analog of the BOCBH core in the CO_2 cycloadduct [**2**H]$^-$ (Scheme 2a). A mere shift of the bridging H^- ion to a terminal position unlocks the rigid ring system and enables a flip about the C–N bond, which brings the (now tricoordinated) B atom into close vicinity to the electron lone-pair of the carbonyl function. Subsequent B–O adduct formation establishes the BNCO ring of [**4**H]$^-$.[46] All in all, we note a pleasantly good agreement between experiment and theory. One seeming inconsistency relates to the CO_2 cycloadduct [**2**H]$^-$. While NMR spectroscopy and X-ray crystallography reveal a dibenzo[*g*,*p*]chrysene periphery for [**2**H]$^-$, both in solution and in the solid state, the corresponding computed anion structure is energetically less favorable by $\Delta G = +16.5$ kcal mol^{-1} relative to a 9,9′-difluorene-type structure (cf. [**4b**H]$^-$ with O instead of N*i*Pr in Scheme 4). However, even this apparent discrepancy can be explained by the following scenario, which draws a coherent picture of all available experimental and theoretical results:[47] A mapping of the molecular surfaces of [**1**H]$^-$ and [**1b**H]$^-$ showed that the B–B bond of the thermodynamically less favorable, less abundant isomer [**1b**H]$^-$ is more easily accessible than for [**1**H]$^-$.[5] This is mainly due to different spatial orientations of the *t*Bu groups relative to the B–B bonds. We assume that the small CO_2 molecule can nevertheless react similarly well with both isomers. The product distribution is thus dictated by the relative abundancies of [**1**H]$^-$ vs. [**1b**H]$^-$ and dominated by the experimentally observed K[**2**H], which, once formed, does not rearrange to the computed global minimum structure.[31] The *i*PrNCN*i*Pr molecule, on the other hand, is so bulky that it entirely neglects the B–B bond and prefers to react with the protruding B–H bond of [**1a**H]$^-$ to afford K[**3**]. The intermediate-sized *i*PrNCO has the option to use a similar reaction trajectory as *i*PrNCN*i*Pr (B–H bond activation yielding K[**5**]). Alternatively, it can perform a CO_2-like B–B bond activation, with the distinct restriction to the sterically less demanding μ-H component [**1b**H]$^-$ in the equilibrium of isomeric starting materials (yielding K[**4**H]). This selectivity for [**1b**H]$^-$ over [**1**H]$^-$ is further enhanced by the fact that the formation of the thermodynamic primary product [**4b**H]$^-$ requires a reaction at the sterically more encumbered C=N bond of *i*PrNCO (cf. Scheme 4).

Conclusion

Interest in μ-(hydrido)diboranes(4) with their electron-precise B–B bonds and bridging H^- ligands goes back many decades, but to date most of the knowledge has come from quantum-chemical calculations on the simplest representative, the elusive anion $[B_2H_5]^-$. It has been suggested that the B–B bond acts as a non-classical electron-donor site, but also that a mere shift of the μ-H atom to a terminal position fundamentally alters the frontier orbitals of the system and generates a H^- donor with a nearby Lewis acidic B center. Experimental insight into the unique properties of the central BHB unit has been hampered by the lack of synthetically accessible (μ-hydrido)diborane(4) derivatives, in which the BHB core is not perturbed by electron-donating or sterically protecting substituents. Our representative K[**1**H] with planarized dibenzo[*g*,*p*]chrysene-type scaffold comes close to this ideal and reacts straightforwardly with various substrates, such as the heterocumulenes CO_2, *i*PrNCO, and *i*PrNCN*i*Pr in either B–B or B–H bond activation reactions. The actual activation scenario is governed by two factors, (i) the steric demand of the substrate molecule and (ii) the ready isomerization of [**1**H]$^-$ with bridging H^- ligand to its isomer [**1a**H]$^-$ with terminal B–H bond: The small CO_2 molecule can still undergo a formal [2+2] cycloaddition with the sterically loaded B–B bond of [**1**H]$^-$, thereby forming a BOCBH heterocycle (K[**2**H]). The bulky substrate *i*PrNCN*i*Pr most easily interacts with the B–H bond of [**1a**H]$^-$ to give the B(sp^3)–B(sp^3) diborane salt K[**3**] with a BNCNB ring. Both B–B and B–H bond activations are observed for the hybrid

substrate *i*PrNCO, leading to the two isomeric and almost isoenergetic products K[**4**H] and K[**5**]. Taken together, it is experimentally demonstrated here for the first time that H^- ligand-supported B–B single bonds show cycloaddition reactivities that would normally be associated with B=B double bonds, thus opening new perspectives for organoborane synthesis.

Acknowledgements

T.T. thanks the Fonds der Chemischen Industrie for a Ph.D. grant. We thank Albemarle Germany GmbH (Frankfurt) for the generous gift of chemicals. Open access funding enabled and organized by Projekt DEAL.

Conflict of interest

The authors declare no conflict of interest.

Keywords: B–B bonds · B–H bonds · bond activation · cycloaddition · diboranes

[1] "C–H Bond Activation and Catalytic Functionalization I & II": *Topics in Organometallic Chemistry*, *Vol. 55*, *56* (Eds.: P. H. Dixneuf, H. Doucet), Springer International Publishing, Cham, **2016**.

[2] W. Kutzelnigg, *Angew. Chem. Int. Ed. Engl.* **1984**, *23*, 272 – 295; *Angew. Chem.* **1984**, *96*, 262 – 286.

[3] Z. L. Wang, H. S. Hu, L. von Szentpály, H. Stoll, S. Fritzsche, P. Pyykkö, W. H. E. Schwarz, J. Li, *Chem. Eur. J.* **2020**, *26*, 15558 – 15564.

[4] H. C. Brown, *Tetrahedron* **1961**, *12*, 117 – 138.

[5] T. Trageser, M. Bolte, H.-W. Lerner, M. Wagner, *Angew. Chem. Int. Ed.* **2020**, *59*, 7726 – 7731; *Angew. Chem.* **2020**, *132*, 7800 – 7805.

[6] a) C. Kleeberg, L. Dang, Z. Lin, T. B. Marder, *Angew. Chem. Int. Ed.* **2009**, *48*, 5350 – 5354; *Angew. Chem.* **2009**, *121*, 5454 – 5458; b) A. Bonet, C. Pubill-Ulldemolins, C. Bo, H. Gulyás, E. Fernández, *Angew. Chem. Int. Ed.* **2011**, *50*, 7158 – 7161; *Angew. Chem.* **2011**, *123*, 7296 – 7299; c) R. D. Dewhurst, E. C. Neeve, H. Braunschweig, T. B. Marder, *Chem. Commun.* **2015**, *51*, 9594 – 9607; d) E. C. Neeve, S. J. Geier, I. A. I. Mkhalid, S. A. Westcott, T. B. Marder, *Chem. Rev.* **2016**, *116*, 9091 – 9161; e) A. B. Cuenca, R. Shishido, H. Ito, E. Fernández, *Chem. Soc. Rev.* **2017**, *46*, 415 – 430.

[7] B. Ruščic, M. Schwarz, J. Berkowitz, *J. Chem. Phys.* **1989**, *91*, 4576 – 4581.

[8] S.-L. Chou, J.-I. Lo, Y.-C. Peng, M.-Y. Lin, H.-C. Lu, B.-M. Cheng, J. F. Ogilvie, *Chem. Sci.* **2015**, *6*, 6872 – 6877.

[9] Isolable derivatives of the C_{2v} or D_{2d} isomers of B_2H_4 were obtained by Tamao et al. through the introduction of two 1,1,3,3,5,5,7,7-octaethyl-*s*-hydrindacen-4-yl (Eind) or 1,1,7,7-tetramethyl-3,3,5,5-tetrapropyl-*s*-hydrindacen-4-yl (MPind) groups, respectively: a) Y. Shoji, T. Matsuo, D. Hashizume, H. Fueno, K. Tanaka, K. Tamao, *J. Am. Chem. Soc.* **2010**, *132*, 8258 – 8260; b) Y. Shoji, S. Kaneda, H. Fueno, K. Tanaka, K. Tamao, D. Hashizume, T. Matsuo, *Chem. Lett.* **2014**, *43*, 1587 – 1589; Yamashita et al. reported a structurally related tetraborane: c) A. Yagi, H. Kisu, M. Yamashita, *Dalton Trans.* **2019**, *48*, 5496 – 5499.

[10] a) R. W. Parry, G. Kodama, *Coord. Chem. Rev.* **1993**, *128*, 245 – 260; b) Y. Wang, B. Quillian, P. Wei, C. S. Wannere, Y. Xie, R. B. King, H. F. Schaefer, P. v. R. Schleyer, G. H. Robinson, *J. Am. Chem. Soc.* **2007**, *129*, 12412 – 12413.

[11] For a recent review article covering corresponding compounds and related subvalent species, see: H. Budy, J. Gilmer, T. Trageser, M. Wagner, *Eur. J. Inorg. Chem.* **2020**, 4148 – 4162.

[12] M.-C. Liu, H.-F. Chen, W.-J. Huang, C.-H. Chin, S.-C. Chen, T.-P. Huang, Y.-J. Wu, *J. Chem. Phys.* **2016**, *145*, 074314.

[13] a) R. L. DeKock, P. Deshmukh, T. P. Fehlner, C. E. Housecroft, J. S. Plotkin, S. G. Shore, *J. Am. Chem. Soc.* **1983**, *105*, 815 – 822; b) P. D. Grebenik, M. L. H. Green, M. A. Kelland, J. B. Leach, P. Mountford, G. Stringer, N. M. Walker, L.-L. Wong, *J. Chem. Soc. Chem. Commun.* **1988**, 799 – 801; c) T. J. Coffy, G. Medford, J. Plotkin, G. J. Long, J. C. Huffman, S. G. Shore, *Organometallics* **1989**, *8*, 2404 – 2409.

[14] a) K. S. Pitzer, *J. Am. Chem. Soc.* **1945**, *67*, 1126 – 1132; b) K. Lammertsma, T. Ohwada, *J. Am. Chem. Soc.* **1996**, *118*, 7247 – 7254; c) D. J. Goebbert, H. Hernandez, J. S. Francisco, P. G. Wenthold, *J. Am. Chem. Soc.* **2005**, *127*, 11684 – 11689.

[15] T. Kaese, H. Budy, M. Bolte, H.-W. Lerner, M. Wagner, *Angew. Chem. Int. Ed.* **2017**, *56*, 7546 – 7550; *Angew. Chem.* **2017**, *129*, 7654 – 7658.

[16] Y. Shoji, T. Matsuo, D. Hashizume, M. J. Gutmann, H. Fueno, K. Tanaka, K. Tamao, *J. Am. Chem. Soc.* **2011**, *133*, 11058 – 11061.

[17] Uncharged and cationic analogs of $[B_2H_5]^-$ are known: a) P. Bissinger, H. Braunschweig, A. Damme, R. D. Dewhurst, T. Kupfer, K. Radacki, K. Wagner, *J. Am. Chem. Soc.* **2011**, *133*, 19044 – 19047; b) S. R. Wang, D. Prieschl, J. D. Mattock, M. Arrowsmith, C. Pranckevicius, T. E. Stennett, R. D. Dewhurst, A. Vargas, H. Braunschweig, *Angew. Chem. Int. Ed.* **2018**, *57*, 6347 – 6351; *Angew. Chem.* **2018**, *130*, 6456 – 6460; c) M. Arrowsmith, J. D. Mattock, S. Hagspiel, I. Krummenacher, A. Vargas, H. Braunschweig, *Angew. Chem. Int. Ed.* **2018**, *57*, 15272 – 15275; *Angew. Chem.* **2018**, *130*, 15493 – 15497; d) T. Brückner, T. E. Stennett, M. Heß, H. Braunschweig, *J. Am. Chem. Soc.* **2019**, *141*, 14898 – 14903; e) U. Schmidt, L. Werner, M. Arrowsmith, A. Deissenberger, A. Hermann, A. Hofmann, S. Ullrich, J. D. Mattock, A. Vargas, H. Braunschweig, *Angew. Chem. Int. Ed.* **2020**, *59*, 325 – 329; *Angew. Chem.* **2020**, *132*, 333 – 337; f) S. Akiyama, M. Yamashita, *Chem. Lett.* **2020**, *49*, 721 – 723.

[18] A. Hübner, Z.-W. Qu, U. Englert, M. Bolte, H.-W. Lerner, M. C. Holthausen, M. Wagner, *J. Am. Chem. Soc.* **2011**, *133*, 4596 – 4609.

[19] A. Hübner, M. Diefenbach, M. Bolte, H.-W. Lerner, M. C. Holthausen, M. Wagner, *Angew. Chem. Int. Ed.* **2012**, *51*, 12514 – 12518; *Angew. Chem.* **2012**, *124*, 12682 – 12686.

[20] A. Hübner, A. M. Diehl, M. Bolte, H.-W. Lerner, M. Wagner, *Organometallics* **2013**, *32*, 6827 – 6833.

[21] A. Hübner, M. Bolte, H.-W. Lerner, M. Wagner, *Angew. Chem. Int. Ed.* **2014**, *53*, 10408 – 10411; *Angew. Chem.* **2014**, *126*, 10576 – 10579.

[22] T. Kaese, A. Hübner, M. Bolte, H.-W. Lerner, M. Wagner, *J. Am. Chem. Soc.* **2016**, *138*, 6224 – 6233.

[23] A. Lorbach, A. Hübner, M. Wagner, *Dalton Trans.* **2012**, *41*, 6048 – 6063.

[24] E. von Grotthuss, A. John, T. Kaese, M. Wagner, *Asian J. Org. Chem.* **2018**, *7*, 37 – 53.

[25] J. Gilmer, H. Budy, T. Kaese, M. Bolte, H.-W. Lerner, M. Wagner, *Angew. Chem. Int. Ed.* **2020**, *59*, 5621 – 5625; *Angew. Chem.* **2020**, *132*, 5670 – 5674.

[26] T. Kaese, T. Trageser, H. Budy, M. Bolte, H.-W. Lerner, M. Wagner, *Chem. Sci.* **2018**, *9*, 3881 – 3891.

[27] Q. Zhao, R. D. Dewhurst, H. Braunschweig, X. Chen, *Angew. Chem. Int. Ed.* **2019**, *58*, 3268 – 3278; *Angew. Chem.* **2019**, *131*, 3302 – 3313.

[28] E. von Grotthuss, M. Diefenbach, M. Bolte, H.-W. Lerner, M. C. Holthausen, M. Wagner, *Angew. Chem. Int. Ed.* **2016**, *55*, 14067 – 14071; *Angew. Chem.* **2016**, *128*, 14273 – 14277.
[29] E. von Grotthuss, S. E. Prey, M. Bolte, H.-W. Lerner, M. Wagner, *Angew. Chem. Int. Ed.* **2018**, *57*, 16491 – 16495; *Angew. Chem.* **2018**, *130*, 16729 – 16733.
[30] E. von Grotthuss, S. E. Prey, M. Bolte, H.-W. Lerner, M. Wagner, *J. Am. Chem. Soc.* **2019**, *141*, 6082 – 6091.
[31] Temperature treatment of Li[**2**H] in [D_8]THF under an atmosphere of CO_2 (sealed NMR tube) resulted in the breaking of the C–O bond with release of CO (detected at $\delta(^{13}C) = 184.9$ ppm) and furnished, among other products, an oligomeric boronic/borinic acid anhydride, which was characterized by X-ray diffraction (Figure S72; for $M^+ = K^+$, an even less selective decomposition was observed by NMR spectroscopy).
[32] a) S. E. Prey, M. Wagner, *Adv. Synth. Catal.* **2021**, *363*, 2290 – 2309; b) M. Frick, J. Horn, H. Wadepohl, E. Kaifer, H.-J. Himmel, *Chem. Eur. J.* **2018**, *24*, 16983 – 16986.
[33] "Nuclear Magnetic Resonance Spectroscopy of Boron Compounds": H. Nöth, B. Wrackmeyer, in *NMR Basic Principles and Progress* (Eds.: P. Diehl, E. Fluck, R. Kosfeld), Springer, Berlin, **1978**.
[34] B. Cordero, V. Gómez, A. E. Platero-Prats, M. Revés, J. Echeverría, E. Cremades, F. Barragán, S. Alvarez, *Dalton Trans.* **2008**, 2832 – 2838.
[35] A. Stoy, J. Böhnke, J. O. C. Jiménez-Halla, R. D. Dewhurst, T. Thiess, H. Braunschweig, *Angew. Chem. Int. Ed.* **2018**, *57*, 5947 – 5951; *Angew. Chem.* **2018**, *130*, 6055 – 6059.
[36] M. Cortijo, R. González-Prieto, S. Herrero, J. L. Priego, R. Jiménez-Aparicio, *Coord. Chem. Rev.* **2019**, *400*, 213040.
[37] M. Hesse, H. Meier, B. Zeeh, *Spektroskopische Methoden in der organischen Chemie*, 8th ed., G. Thieme Verlag, Stuttgart, New York, **2012**.
[38] R. Rieger, K. Müllen, *J. Phys. Org. Chem.* **2010**, *23*, 315 – 325.
[39] A. Bax, J. A. Ferretti, N. Nashed, D. M. Jerina, *J. Org. Chem.* **1985**, *50*, 3029 – 3034.
[40] K. Tominaga, Y. Sakamoto, Y. Fujimaki, M. Takekawa, S. Ohshima, *Polycyclic Aromat. Compd.* **2010**, *30*, 274 – 286.
[41] We also prepared derivatives of [**3**]$^-$ by replacing *i*PrNCN*i*Pr with (Me_3Si)NCN($SiMe_3$) or *p*TolNCN*p*Tol (see the Supporting Information for full details).
[42] a) K. E. Krahulic, G. D. Enright, M. Parvez, R. Roesler, *J. Am. Chem. Soc.* **2005**, *127*, 4142 – 4143; b) A. Kausamo, H. M. Tuononen, K. E. Krahulic, R. Roesler, *Inorg. Chem.* **2008**, *47*, 1145 – 1154.
[43] a) N. Schulenberg, S. Litters, E. Kaifer, H.-J. Himmel, *Eur. J. Inorg. Chem.* **2011**, 2657 – 2661; b) A. Widera, H. Wadepohl, H.-J. Himmel, *Angew. Chem. Int. Ed.* **2019**, *58*, 5897 – 5901; *Angew. Chem.* **2019**, *131*, 5957 – 5961; c) E. Fırıncı, R. Fırıncı, R. Sevinçek, M. Aygün, Y. Şahin, *Chem. Commun.* **2020**, *56*, 9807 – 9810.
[44] a) M. Radius, E. Sattler, H. Berberich, F. Breher, *Chem. Eur. J.* **2019**, *25*, 12206 – 12213; b) C. Chen, C. G. Daniliuc, C. Mück-Lichtenfeld, G. Kehr, G. Erker, *J. Am. Chem. Soc.* **2020**, *142*, 19763 – 19771.
[45] Calculations were performed at the PBE0D/TZVP level of theory with the SMD polarized continuum model for solvation in THF. Counter cations and *t*Bu groups have been omitted for simplicity.
[46] In the case of the CO_2 cycloadduct [**2**H]$^-$, this rearrangement sequence is suppressed by the rigid dibenzo[*g*,*p*]chrysene scaffold, and therefore K[**2**H] is an isolable compound.
[47] Counter-cation effects are not included but may also play a role.

Manuscript received: March 9, 2021
Accepted manuscript online: March 19, 2021
Version of record online: May 3, 2021

